1995

# A Simplified Turbulence Model for Describing Airflow in Ceiling Slot-ventilated Enclosures

Steven J. Hoff
*Iowa State University*, hoffer@iastate.edu

# A SIMPLIFIED TURBULENCE MODEL FOR DESCRIBING AIRFLOW IN CEILING SLOT-VENTILATED ENCLOSURES

S. J. Hoff

**ABSTRACT.** *A numerical model was developed to predict flow occurring with opposing plane-wall ceiling jets representative of slot-ventilated livestock facilities. This model, termed the BETA model, was evaluated by comparing predicted axial and animal occupied zone (AOZ) velocity distributions with a low Reynold's Number turbulence model (LBLR) and a laminar model (LAM). In addition, the BETA model results were compared with experimental results from a laboratory-scale test chamber. For opposing plane-wall ceiling jets, the predominant gradient in turbulent viscosity was predicted to occur in the vertical direction. An effective viscosity was defined as a function of the inlet Reynold's Number ($Re_H$) and normalized vertical height from the floor. The effective viscosity was used to selectively augment the laminar viscosity in the Navier-Stoke's equation. Predicted comparisons between BETA and the LBLR models showed negligible differences for ventilating conditions between $Re_H$ of 35,032 and 11,752. Comparison with experimentally measured axial velocity decay indicated that the BETA model reproduced ceiling jet development as well as the LBLR model.*
***Keywords.*** *Model, Ventilation, Turbulence.*

Numerical models describing airflow and the turbulent distributions of mass, momentum, and energy have been successfully developed for many ventilation situations. The models developed to date have focused on describing the spatial distribution of turbulent kinetic energy and the dissipation of turbulent kinetic energy throughout the flow field. The solution to all equations requires computing facilities that provide substantial storage and computational speed.

One model approach that holds promise for livestock building airflow situations uses the laminar version of the Navier-Stokes equation in conjunction with spatial variations of turbulent viscosity determined from the Lam-Bremhorst low Reynold's Number (LBLR) turbulence model (Lam and Bremhorst, 1981). Such a model may enable adequate prediction of airflow pattern and velocity distributions throughout the flow regime without the computational overhead required for the LBLR model.

Development of such a model would involve determining a suitable relation for the distribution of turbulent viscosity by use of the LBLR model. A predictable distribution of turbulent viscosity could be used directly in a modified form of the laminar Navier-Stokes equations. Source terms associated with a changing viscosity could then be incorporated into the momentum equations. This procedure, if successful, would substantially reduce the computational expense of describing turbulent airflow for slot-ventilated livestock facilities since differential equations describing turbulence would no longer be necessary.

In order to evaluate this modeling approach, the objectives of this study were to: 1) develop a simplified turbulence model that adequately describes airflow pattern and the spatial distribution of mass and momentum in a ceiling slot-ventilated livestock facility with opposing ceiling jets (fig. 3); and 2) evaluate the success of the model by comparing the simplified model results with LBLR model results and empirical data collected in a laboratory-scale chamber.

A model, if successfully developed, would allow the solution of mathematical simulations on portable desktop computers and still retain the predictive capabilities of more sophisticated models.

## LITERATURE REVIEW

Several researchers have used mathematical models to simulate airflow in livestock facilities. Timmons et al. (1980) applied an inviscid two-dimensional model to a slot-ventilated livestock facility. Janssen and Krause (1988) applied a two-dimensional model that described velocity, temperature, and contaminant distributions in slot-ventilated livestock facilities. The model used an augmented laminar viscosity to account for turbulence effects in the building. Choi et al. (1987, 1988, 1990) applied the isothermal fully turbulent k-ε model to a two-dimensional slot-ventilated enclosure. They investigated the distributions of velocity and contaminants with and without obstructions and found very reasonable agreements with experimental results. Hoff et al. (1992) developed a three-dimensional model for describing buoyancy-affected airflow in ceiling slot-ventilated livestock facilities. The model was based on the LBLR turbulence model proposed by Lam and Bremhorst (1982). Comparison with experimentally measured temperature and velocity distributions showed that the model adequately described

Article was submitted for publication in May 1994; reviewed and approved for publication by the Structures and Environment Div. of ASAE in December 1994.

Journal Paper No. J-15715 of the Iowa Agriculture and Home Economics Experiment Station, Ames, Iowa. Project No. 3140.

The author is **Steven J. Hoff**, ***ASAE Member Engineer,*** Associate Professor, Agricultural and Biosystems Engineering Dept., Iowa State University, Ames, IA 50011; e-mail: <hoffer@iastate.edu>.

  

mass, momentum, and energy distributions (Hoff et al., 1994).

Two major turbulence models have been developed that involve computation of turbulent kinetic energy (k) and dissipation rate (ε). The Fully Turbulent k-ε model (FTKE) was developed by Harlow and Nakayama (1969) and refined by Launder and Spalding (1972). The FTKE assumes that all points within the solution grid exist in a region of fully turbulent flow ($y^+ > 11.63$). For regions where this requirement is not met, such as solid boundaries, wall-functions are used (Patankar and Spalding, 1970; Launder and Spalding, 1974).

The low Reynold's Number k-ε model (LRKE) was developed (Launder and Spalding, 1972) to eliminate the need for special treatments, such as wall-functions, in regions where fully turbulent conditions do not exist. The LRKE model requires a more refined grid, relative to the FTKE model, and thus has been limited to those cases where the FTKE cannot be used.

Lam and Bremhorst (1981) developed a LRKE model that retains the features of the FTKE model and is applicable to near-wall boundaries. In this version, if the flow is indeed turbulent, the model becomes computationally similar to the well-tested FTKE model.

## LBLR Model

The LBLR model developed by Lam and Bremhorst (1981) defines the effective viscosity as (all symbols defined in nomenclature):

$$\mu_{eff} = \mu_l + \mu_t \tag{1}$$

where

$\mu_l$ = laminar viscosity

$$\mu_t = \rho\, c_\mu\, f_\mu \frac{k^2}{\varepsilon}$$

The turbulent viscosity varies throughout the flow field and is a function of the spatial distribution of turbulent kinetic energy (k) and the dissipation rate of turbulent kinetic energy (ε). The spatial distribution of k and ε are described by the following equations:

$$\frac{\partial(\rho\, u_i\, k)}{\partial x_i} = \frac{\partial}{x_i}\left(\Gamma \frac{\partial k}{\partial x_i}\right) + \mu_t\, \rho\, \overline{P} - \rho\varepsilon \tag{2}$$

$$\frac{\partial(\rho\, u_i\, \varepsilon)}{\partial x_i} = \frac{\partial}{\partial x_i}\left(\Gamma \frac{\partial \varepsilon}{\partial x_i}\right) + \frac{\rho\varepsilon}{k}\left(c_1 f_1 \mu_t\, \overline{P} - c_2 f_2 \varepsilon\right) \tag{3}$$

and are solved simultaneously with the turbulent mass and momentum equations. The LBLR model has been described by Hoff et al. (1992) for slot-ventilated livestock facilities. The equations describing isothermal airflow are shown in table 1. In general, six partial differential equations must be solved simultaneously to achieve a converged solution.

Boundary conditions were assigned according to the recommendations given by Patel et al. (1985). In general, at all solid boundaries the turbulent kinetic energy (k) was set equal to zero and the normal gradient of the dissipation of turbulent kinetic energy ($\partial\varepsilon/\partial\eta$) was set equal to zero. In addition, u, v, and w components of velocity were set equal to zero at all solid boundaries. At the inlet, the slot-width was set according to the estimated vena contracta ($h_{model} = C_d \times h_{physical}$) resulting in an inlet axial velocity of:

$$U_{in} = \frac{Q}{(C_d\, h_{physical})\, W} \tag{4}$$

The vertical (v) and transverse (w) velocities at the inlet were set equal to zero. The inlet k and ε values were based on the inlet velocity determined from equation 4:

$$k_{in} = 0.005\, U_{in}^{0.5} \tag{5}$$

$$\varepsilon_{in} = 0.33\, k_{in}^{1.5} \tag{6}$$

**Table 1. LBLR model**

**Source Terms and Auxiliary Equations**

| $\phi$ | $\Gamma_\phi$ | $S_\phi$ |
|---|---|---|
| 1 | 0 | 0 |
| u | $\mu_{eff}$ | $\frac{\partial \mu_t}{\partial x_i}\frac{\partial \mu_i}{\partial x} - \frac{\partial P'}{\partial x}$ |
| v | $\mu_{eff}$ | $\frac{\partial \mu_t}{\partial x_i}\frac{\partial u_i}{\partial y} - \frac{\partial P'}{\partial y}$ |
| w | $\mu_{eff}$ | $\frac{\partial \mu_t}{\partial x_i}\frac{\partial u_i}{\partial z} - \frac{\partial P'}{\partial z}$ |
| k | $\mu_l + \frac{\mu_t}{\sigma_k}$ | $\mu_t\, \rho\,(\overline{P} - \varepsilon)$ |
| ε | $\mu_l + \frac{\mu_t}{\sigma_\varepsilon}$ | $\frac{\rho\,\varepsilon}{k}\left(c_1 f_1 \mu_t\, \overline{P} - c_2 f_2 \varepsilon\right)$ |

**Auxiliary Relations**

$\overline{P} = \left(\frac{\partial u_i}{\partial x_j} + \frac{\partial u_j}{\partial x_i}\right)\frac{\partial u_i}{\partial x_j}$ $\quad P' = P + \frac{2}{3}k$

$\mu_t = c_\mu \rho f_\mu \frac{k^2}{\varepsilon}$ $\quad f_\mu = (1.0 - e^{-A_\mu R_k})^2\left(1.0 + \frac{A_t}{R_t}\right)$

$f_1 = 1.0 + \left(\frac{A_{cl}}{f_\mu}\right)^3$ $\quad f_2 = 1.0 - e^{-R_t^2}$

$R_k = \frac{k^{0.5}\rho y_p}{\mu_l}$ $\quad R_t = \frac{k^2\rho}{\mu_l \varepsilon}$

$c_1 = 1.44$ $\quad A_\mu = 0.0165$
$c_2 = 1.92$ $\quad A_t = 20.50$
$c_\mu = 0.09$ $\quad A_{cl} = 0.05$

$\sigma_t = 0.90$
$\sigma_k = 1.00$
$\sigma_\varepsilon = 1.30$

## LAMINAR MODEL (LAM)

The LAM tested was the Navier-Stoke's equation for incompressible fluid flow (Kays and Crawford, 1980). Boundary conditions were set such that velocities in the x, y, and z directions (u, v, and w, respectively) were set to zero at all solid boundaries.

## BETA MODEL DEVELOPMENT

The BETA model developed in this study is based on a relation that describes the spatial distribution of turbulent kinetic energy and hence eliminates the need for including equations 2 and 3 in the solution technique. Data from simulated airflow for a specified ventilating arrangement was used to develop a relation describing the spatial distribution of turbulent viscosity. The turbulent viscosity was then used in the laminar Navier-Stokes equations. Appropriate source terms from the turbulence expressions were retained. Thus, the model developed for this study combines the augmented laminar model and the LBLR model.

Model development required an analysis of the turbulent viscosity distribution predicted with the LBLR model. The augmented viscosity ($\mu_t/\mu_l$) as a function of distance from the floor is shown in figure 1, as average values across horizontal planes in the chamber. Figure 1 shows a fairly consistent pattern and suggests that scaling results using the inlet Reynold's Number based on building height ($Re_H$) may be appropriate. The turbulence factors shown in figure 1 were divided by $Re_H$ and these results are shown in figure 2. In general, for $Re_H$ greater than 17,000 (ACH = 35.0), a reasonable similarity exists for BETA/$Re_H$ as a function of distance (y/H) from the floor. At lower ventilation rates (23.5 and 15.0 ACH) and regions close to the floor (y/H < 0.45), the similarity pattern is not seen. It is unclear why this deviation exists.

The results shown in figure 2 were used as a basis for the simplified model. That is, the laminar viscosity in the LAM model was augmented as a function of normalized distance from the floor. From the results shown in figure 2, the regression equation describing BETA/$Re_H$ as a function of y/H becomes:

$$\frac{\beta}{Re_H} = -27.6 + 13{,}225\left(\frac{y}{H}\right) - 92{,}870\left(\frac{y}{H}\right)^2 + 294{,}915\left(\frac{y}{H}\right)^3 - 461{,}395\left(\frac{y}{H}\right)^4 + 346{,}255\left(\frac{y}{H}\right)^5 - 200.18\left(\frac{y}{H}\right)^6 \quad (7)$$

where

$$\beta = \frac{\mu_t}{\mu_l} = \text{augmented viscosity}$$

$$Re_H = \frac{\rho Q H}{h(2L)\mu_l}$$

The turbulent viscosity was then set according to:

$$\mu_t = \frac{\beta}{Re_H} Re_H \mu_l \quad (8)$$

Resulting in an effective viscosity of:

$$\mu'_{eff} = \mu_l \left(\frac{\beta}{Re_H} Re_H + 1.0\right) \quad (9)$$

Equation 9 represents the proposed distribution of viscosity in a ceiling slot-ventilated chamber incorporating opposing plane-wall jets. Augmented viscosity is assumed to depend only on the vertical location within the chamber.

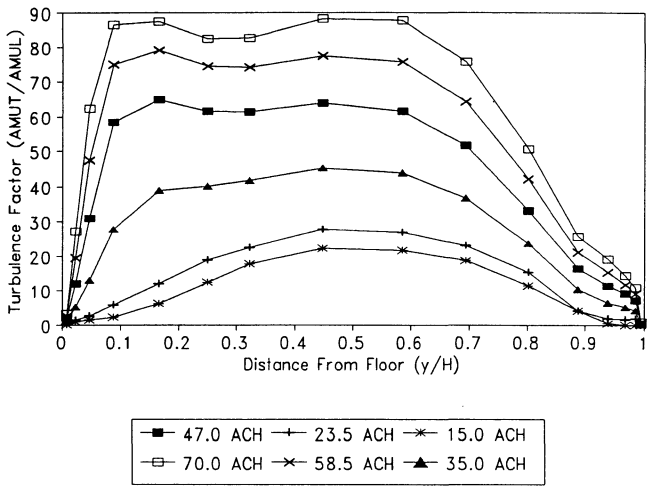


**Figure 1–Turbulence factor as a function of the vertical distance from the floor. Turbulence factor is defined as the calculated turbulent viscosity from the LBLR model divided by the laminar viscosity; values are the averages at each vertical location from the floor.**

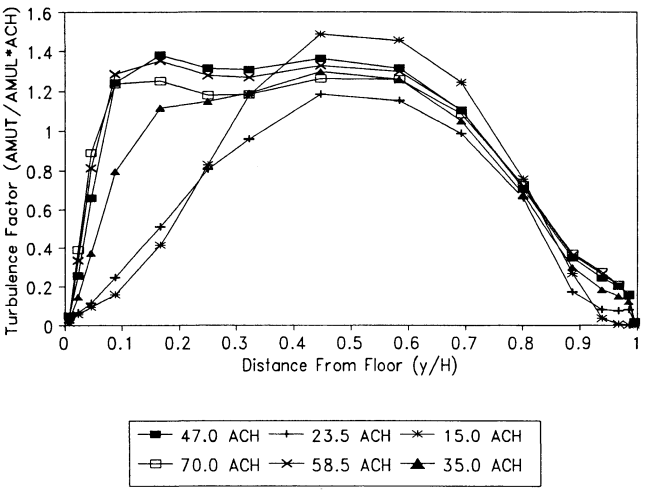


**Figure 2–Turbulence factor divided by the building air exchange rate as a function of vertical distance from the floor. Values presented are the averages of each horizontal plane associated with each vertical location.**

Table 2. BETA model

| Source Terms and Auxiliary Equations | | |
|---|---|---|
| $\phi$ | $\Gamma_\phi$ | $S_\phi$ |
| 1 | 0 | 0 |
| u | $\mu'_{eff}$ | $\frac{\partial \mu_t}{\partial y}\frac{\partial v}{\partial x} - \frac{\partial P}{\partial x}$ |
| v | $\mu'_{eff}$ | $\frac{\partial \mu_t}{\partial y}\frac{\partial v}{\partial y} - \frac{\partial P}{\partial y}$ |
| w | $\mu'_{eff}$ | $\frac{\partial \mu_t}{\partial y}\frac{\partial v}{\partial z} - \frac{\partial P}{\partial z}$ |

| Auxiliary Relations | |
|---|---|
| $\mu'_{eff} = \mu_l\left(\frac{\beta}{Re_H} Re_H + 1.0\right)$ | $\mu_t = \mu_l \frac{\beta}{Re_H} Re_H$ |

### Source Term Adjustments

The simplified model allows for vertical gradients in turbulent viscosity and thus the source terms from table 1 involving these terms must be included. The simplified governing differential equations and source terms are shown in table 2.

### Boundary Conditions

The boundary conditions were assigned in a manner analogous to the LAM model. At each solid boundary, u, v, and w velocities were set to zero. At the inlet, u was set according to equation 4 with v and w set to zero.

## Numerical Grid and Solution Technique

The numerical grid used for this study was 25 × 18 × 10 for the x, y, and z-directions, respectively. Grid points in the x and z directions were spaced evenly throughout, while grid points in the y direction were nonuniform. In the y-direction, grid points were concentrated near the ceiling-slot region and near the floor region. Spacings were governed by a geometric progression factor of about 1.8 to alleviate stability problems associated with high aspect ratio control-volumes (Kuehn, 1990). The overall grid used was coarse. The nonuniform grid spacing in the y direction concentrated grid points where large gradients were expected (i.e., ceiling-jet profile), which resulted in an efficient use of a limited grid (Patankar, 1980).

The governing differential equations were solved using the control-volume based numerical scheme developed by Patankar and Spalding (1972) and summarized by Patankar (1980). All equations were solved simultaneously using underrelaxation techniques in a purely iterative line-by-line sweeping fashion (Patankar, 1980). The SIMPLER algorithm developed by Patankar (1980) was used. This algorithm represents a revised version of the previously used SIMPLE algorithm (Patankar and Spalding, 1972). All solutions were performed on a Unix-based workstation (DEC5000 PXG; Digital Equipment, Inc.).

## Experimental Comparison

The experimental set-up that was mathematically modeled and used for experimental tests is shown in figure 3. Air enters the chamber through continuous slots adjacent to the chamber ceiling. The slots are located on opposing sides and hence the following results are specific to opposing plane-wall jets.

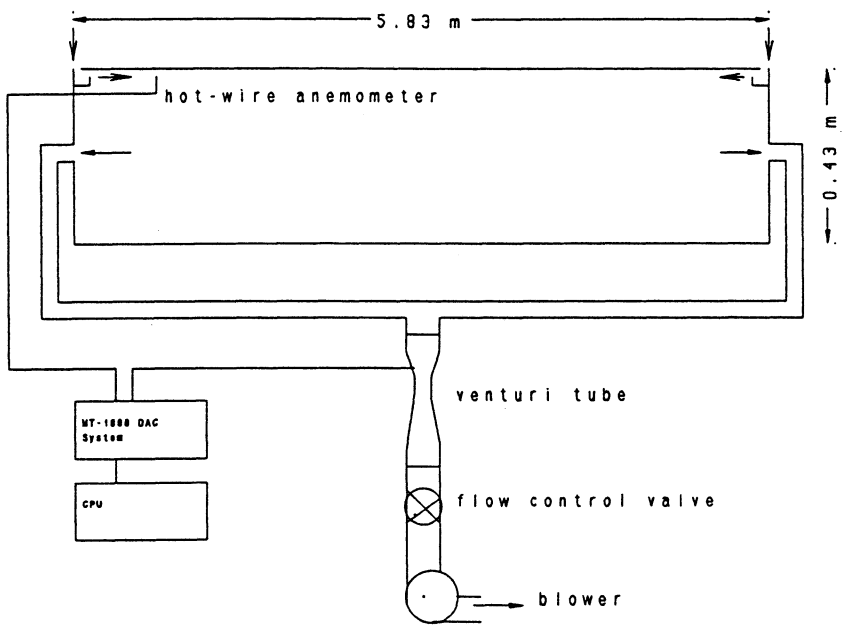


**Figure 3–Experimental chamber used to verify LBLR and BETA model performance. Ventilating conditions for experimental tests are given in table 3.**

The experimental chamber represents a 1:6 geometric scale physical model of the small-pen grower unit at the Swine Nutrition and Management Research Center at Iowa State University. Chamber dimensions were 0.445 × 1.778 × 1.22 m, as shown in figure 3. The slot-width was held constant at 6.4 mm. Mass flow through the chamber was monitored with a venturi tube transducer (model 2020; TSI, Inc.) and adjusted to deliver the required ventilation rate given in table 3. Air velocity was measured with a hot-wire anemometer (model 1212-60; TSI, Inc.).

The anemometer was positioned within the chamber through access holes located on the side of the chamber (fig. 3). Air velocities were sampled at 5 Hz for a 150-s duration. The recorded velocities represent the time-averaged values. Mass flow and air velocity were interfaced with an automated data acquisition system (model MT-1000; Measurement Techniques, Inc.). The chamber air exchange rate shown in table 3 pertains to the 1:6 scale chamber, and can not be directly related to air exchange rates in a full-scale production facility. Recent results for slot-ventilated enclosures (Adre and Albright, 1994) provide guidelines for scaling the test chamber results to full-scale production facilities.

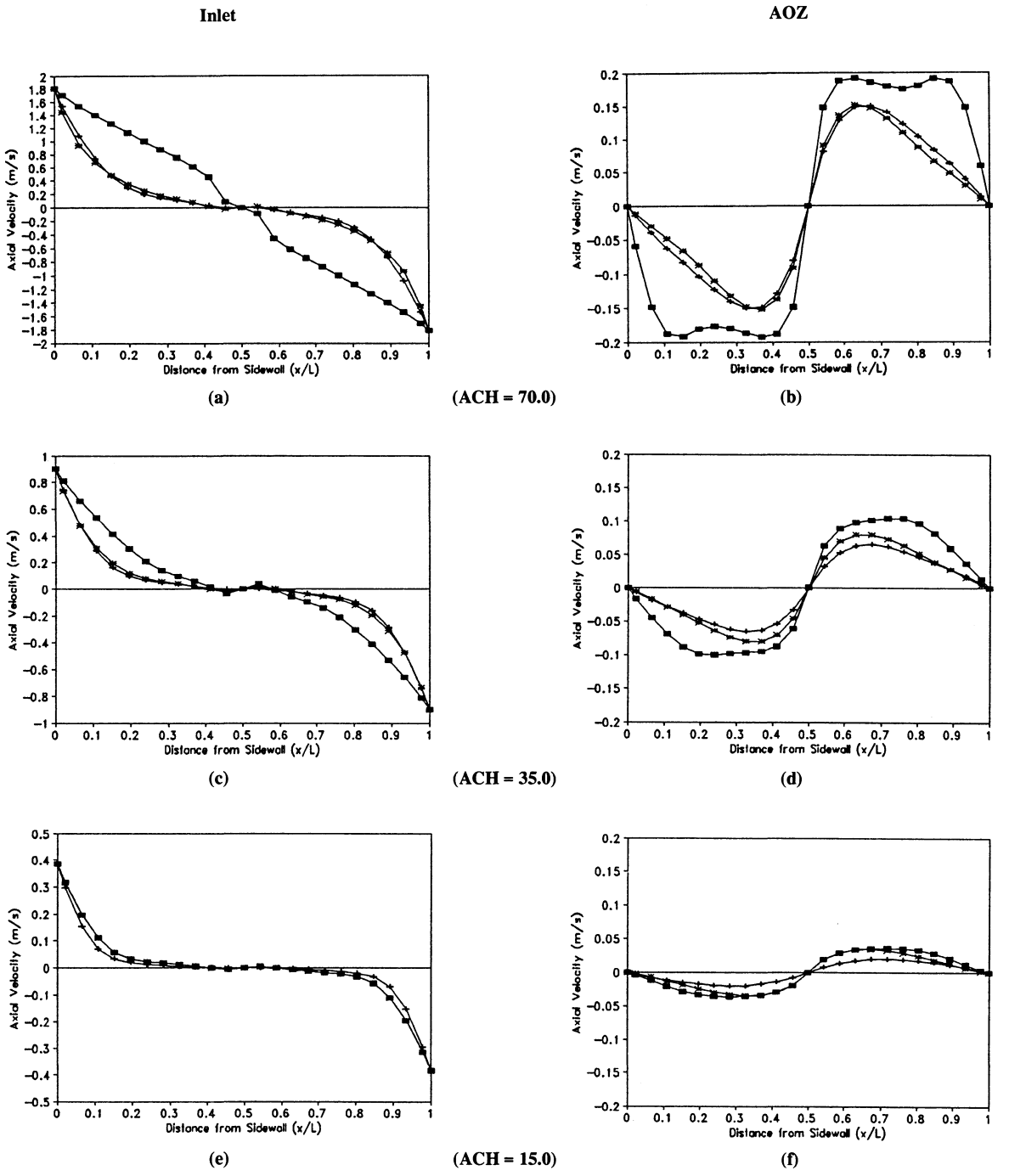


**Figure 4–Axial variation in velocity from (■) LAM, (+) BETA, and (*) LBLR models at the inlet (a, c, and e) and AOZ (b, d, and f) for ventilating conditions four (a, b), six (c, d), and three (e, f).**

Table 3. Ventilating conditions used to verify LBLR and BETA model performances

| Run | ACH ($h^{-1}$) | Q ($m^3/s$) | $Re_h$ | $Re_H$ |
|---|---|---|---|---|
| 1 | 47.0 | 0.012 | 325. | 23,523. |
| 2 | 23.5 | 0.006 | 162. | 11,752. |
| 3 | 15.0 | 0.004 | 103. | 7,461. |
| 4 | 70.0 | 0.018 | 484. | 35,032. |
| 5 | 58.5 | 0.015 | 404. | 29,283. |
| 6 | 35.0 | 0.009 | 241. | 17,470. |

## RESULTS AND DISCUSSION

The model was validated by comparing predicted and measured results from a ceiling slot-ventilated enclosure (fig. 3). The ventilation airflow pattern is three-dimensional, with opposing plane-wall jets flowing along the ceiling. The model was validated at the six ventilating conditions indicated in table 2, which resulted in Reynold's Numbers based on building height ($Re_H$) between 7,500 and 35,000. Results obtained from the BETA model developed in this study were compared to results from the LBLR and LAM models. Where appropriate, experimental results from the test chamber shown in figure 3 were used for comparison.

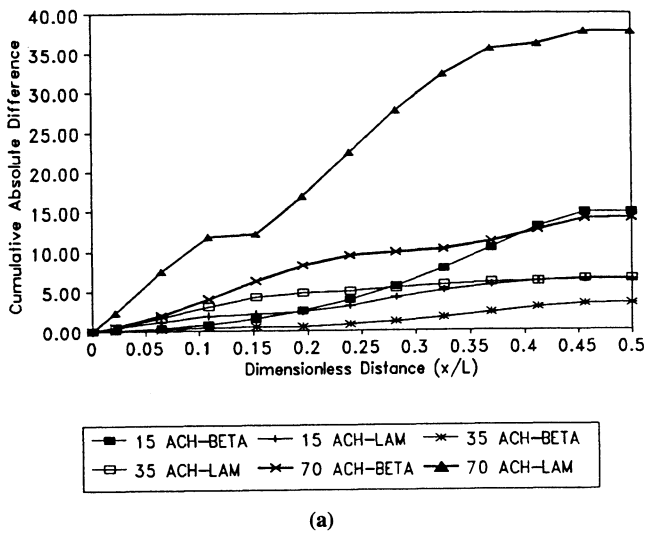


(a)

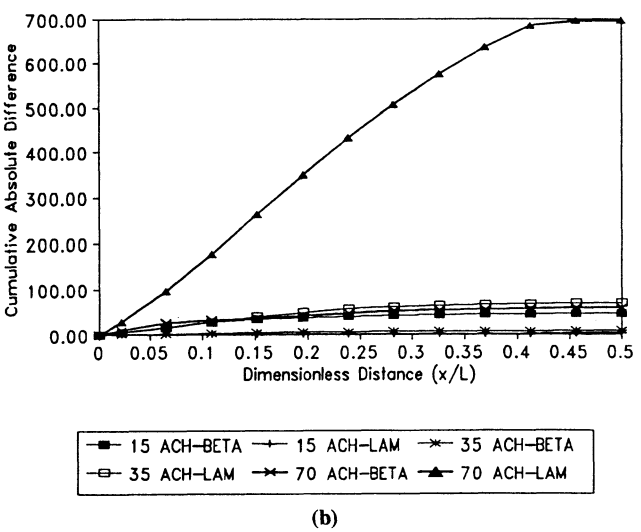


(b)

**Figure 5–Cumulative difference (percent) between the LBLR and the Beta and LAM models for ventilating conditions three, six, and four. Cumulative differences presented at (a) animal-level (y/H = 0.05) and (b) inlet (y/H = 0.99).**

Table 4. Difference between predicted axial velocity decay in the x-direction (m/s) from LBLR model and the BETA and LAM models for ventilating condition four (70 ACH)*

| x/L | LBLR | BETA | Δ% | Σ(Δ%) | LAM | Δ% | Σ(Δ%) |
|---|---|---|---|---|---|---|---|
| 0.000 | 1.806 | 1.806 | 0.0 | 0.0 | 1.806 | 0.0 | 0.0 |
| 0.022 | 1.449 | 1.537 | 9.8 | 9.8 | 1.708 | 28.8 | 28.8 |
| 0.065 | 0.936 | 1.078 | 15.8 | 25.6 | 1.542 | 67.3 | 96.1 |
| 0.109 | 0.673 | 0.733 | 6.6 | 32.2 | 1.403 | 81.0 | 177.2 |
| 0.152 | 0.492 | 0.470 | -2.4 | 34.6 | 1.267 | 86.1 | 263.3 |
| 0.196 | 0.357 | 0.299 | -6.4 | 41.0 | 1.133 | 86.2 | 349.5 |
| 0.239 | 0.257 | 0.203 | -6.0 | 47.0 | 1.000 | 82.6 | 432.0 |
| 0.283 | 0.185 | 0.148 | -4.1 | 51.1 | 0.871 | 76.2 | 508.2 |
| 0.326 | 0.132 | 0.110 | -2.5 | 53.6 | 0.746 | 68.1 | 576.3 |
| 0.370 | 0.081 | 0.073 | -1.0 | 54.5 | 0.619 | 59.7 | 636.1 |
| 0.413 | 0.023 | 0.035 | 1.3 | 55.8 | 0.460 | 48.5 | 684.6 |
| 0.456 | 0.002 | 0.001 | 2.4 | 58.3 | 0.087 | 12.0 | 696.6 |
| 0.500 | 0.000 | 0.000 | 0.0 | 58.3 | 0.000 | 0.0 | 696.9 |

* Percent difference (Δ %) and cumulative absolute difference [ Σ(Δ%)] are defined by eqs. 10 and 11.

### MODEL COMPARISON: AXIAL AND AOZ VELOCITIES

Ventilating conditions four, six, and three ($Re_H$ = 35,032, 1,7470, and 11,752, respectively) were modeled using the test chamber (fig. 3) and axial velocity predictions were compared. Figure 4 summarizes the predicted axial velocity decay and velocity in the animal-occupied zone (AOZ). For each plot, results generated

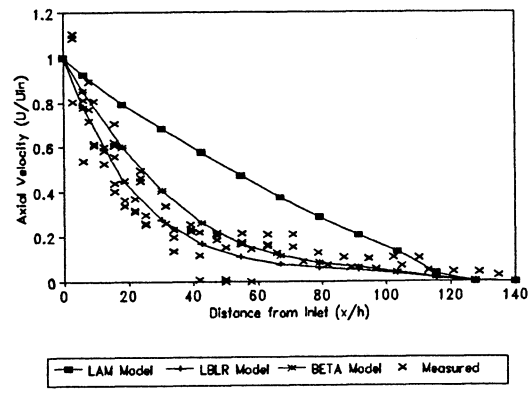


(a)

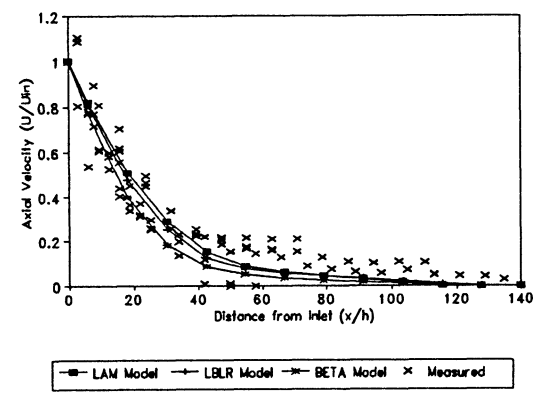


(b)

**Figure 6–Comparison between measured axial velocity decay and predicted results from LAM, LBLR, and BETA models at (a) 47.0 ACH and (b) 15.0 ACH.**

from the (■) LAM, (*) LBLR, and (+) BETA models were compared.

In general, the simplified BETA model predicted axial velocity decay and AOZ velocity as well as the LBLR model. The BETA model's retention of the exponential decay in axial velocity is evident (fig. 4). Maximum differences between the LBLR and BETA model predictions were negligibly small for all cases presented. The results presented in figure 4 suggest that, for the test chamber modeled, i.e., opposing plane-wall ceiling jets, the greatly simplified BETA model can be used as a replacement for the more complete LBLR model. The comparisons between the LBLR and BETA model results shown in figure 3 indicate that the effective viscosity relation proposed in figures 1 and 2 was appropriate.

The importance of including the turbulence features retained in the BETA model is indicated in figure 4 by the poorer predictions of axial and AOZ velocities as $Re_H$ increases by the LAM model. Retaining the turbulent nature of the airflow is important for accurate prediction; the BETA model apparently does so adequately, compared with the LAM model.

The BETA and LAM model results were compared directly with the LBLR predicted results for ventilating conditions three, six, and four. For comparative purposes, two parameters were defined to describe differences between the BETA and LAM models relative to the LBLR model. The percent difference:

$$(\Delta\%)_i = \frac{(U_{model} - U_{LBLR})_i}{U_{in}}(100) \qquad (10)$$

where

$U_{model}$ = x-direction velocity from either the BETA or LAM model (m/s)

$U_{LBLR}$ = x-direction velocity from LBLR model (m/s)

$U_{in}$ = inlet velocity (m/s)

i = location of interest

and cumulative absolute difference:

$$\sum(\Delta\%)_i = \sum_{i=1}^{N}\left[\frac{|U_{model} - U_{LBLR}|_i}{U_{in}}(100)\right] \qquad (11)$$

where N is the total number of locations modeled and were used to assess differences between the models. The cumulative absolute difference was used to highlight regions in the flow field where large comparative errors existed. Figure 5 shows the cumulative absolute difference between the LBLR model and the BETA and LAM models for the AOZ (fig. 5a) and axial velocity decay (fig. 5b) regions.

The inability of the LAM model to adequately predict AOZ (fig. 5a) and axial velocity (fig. 5b) at 70 ACH is clearly evident in figure 5. The cumulative absolute differences far exceeded those predicted with the BETA model. Table 4 summarizes the differences at 70 ACH. The BETA model yielded a maximum difference of 15.8%, whereas the LAM model yielded differences up to 86.2%. Despite the fact that the BETA model requires no additional differential equations relative to the LAM model, its predictive capability is quite reasonable.

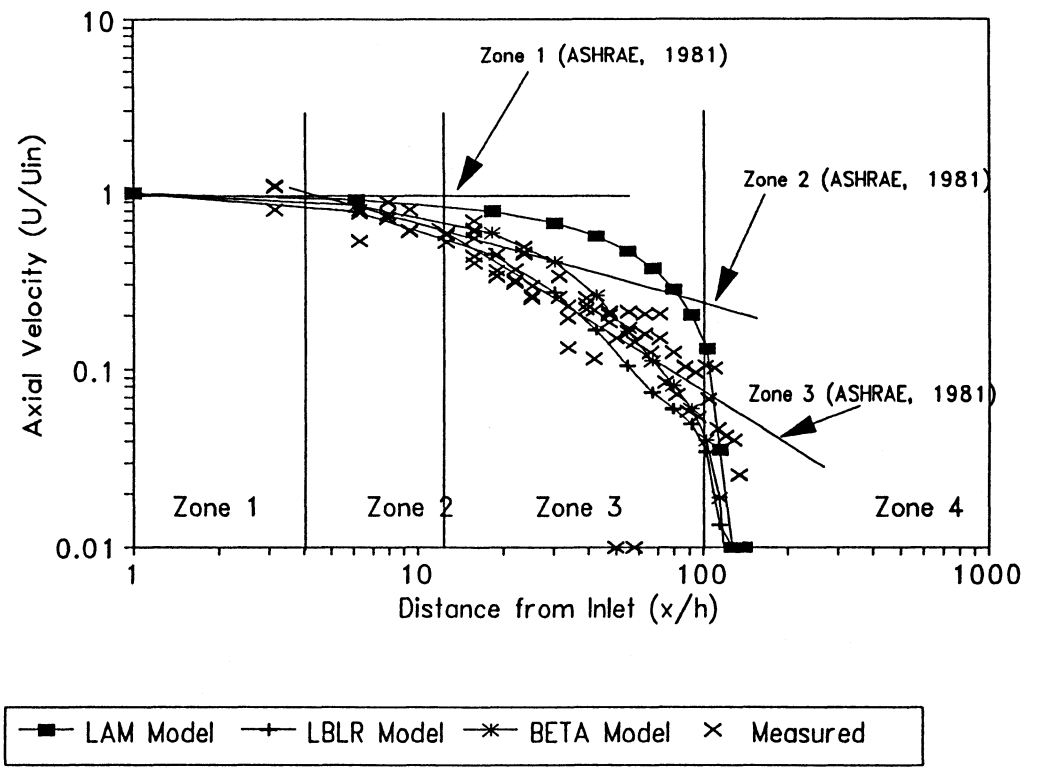


**Figure 7–Comparison between axial velocity decay predictions in jet zones defined by ASHRAE (1993). Data pertains to ventilating condition two (47.0 ACH).**

## Experimentally Measured Results: Axial Velocity Decay

To further verify the BETA model, results were compared with experimentally measured data from the test chamber shown in figure 3. Figures 6 through 9 compare the BETA, LBLR, and LAM model results with experimentally measured results from the test chamber. Figures 6 and 7 compare axial velocity decay and figures 8 and 9 compare vertical jet spread at three axial locations from the inlet.

Figure 6 compares measured axial velocity decay with predicted results from the (■) LAM, (+) LBLR, and (*) BETA models for ventilating conditions one (fig. 6a) and three (fig. 6b). At relatively high $Re_H$ levels (fig. 6a), the BETA and LBLR models adequately predicted the axial velocity decay, whereas the LAM model overpredicted axial velocity. At relatively low inlet $Re_H$ levels (fig. 6b) all three models predicted the measured observations well. Thus, the BETA model is able to accommodate changes from near-laminar to highly turbulent ventilating conditions.

ASHRAE (1993) and Awbi (1992) have defined four observable zones associated with plane-wall jets. Zone 1, the potential core region, extends to nearly 4 effective diameters downstream from the inlet; Zone 2, the characteristic decay region, extends from 4 to about 10 effective diameters; Zone 3, the axisymmetric decay region, extends from 10 to 100 effective diameters; and Zone 4, the terminal region, extends a few effective diameters beyond Zone 3. Figure 7 superimposes the four jet zones described above and the dimensionless profiles for the results shown in figure 6. Clearly, the BETA and LBLR models agree with the empirical information from the ventilation chamber. The LAM model was unsuccessful in predicting axial velocity decay, especially in Zone 3.

As shown in figures 6 and 7, the simplified BETA model adequately reproduced the turbulent features of the developing wall jet and can be used in lieu of the more cumbersome LBLR model. However, these results are only applicable to the ventilating conditions identified in table 3 as applied to the ventilating chamber shown in figure 3. Further research would be needed to develop an applicable database for $\beta/Re_H$ relations for other ventilating arrangements.

## Model Comparison: Vertical Jet Spread

Figure 8 summarizes the LBLR, BETA, and LAM model predictions of vertical jet spread for ventilating conditions three, six, and four. These results are limited to vertical heights between y/H = 0.87 and 1.00, to highlight

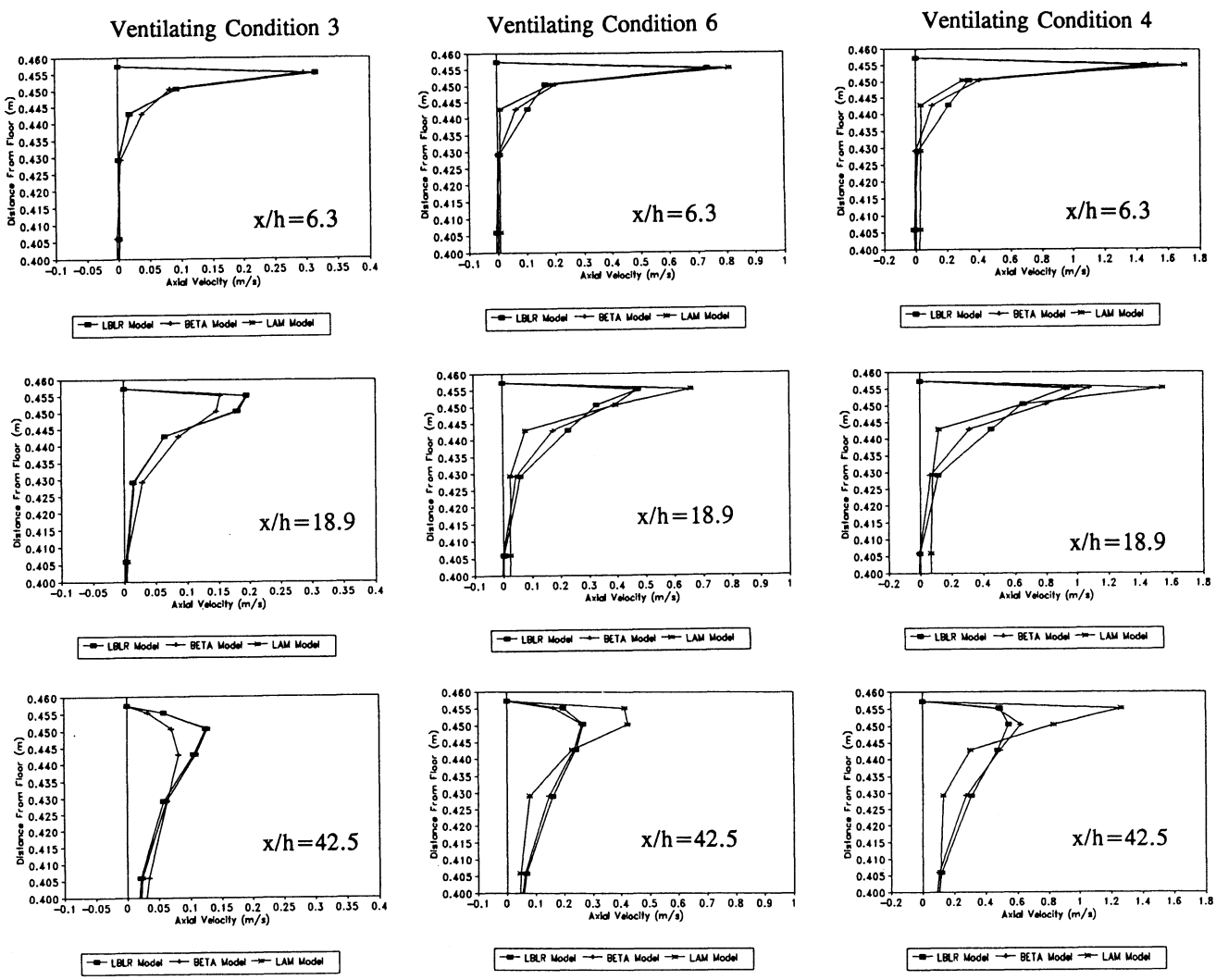


**Figure 8–Vertical jet spread for ventilating conditions three, six, and four at axial locations of x/h = 6.3, x/h = 18.9, and x/h = 42.5.**

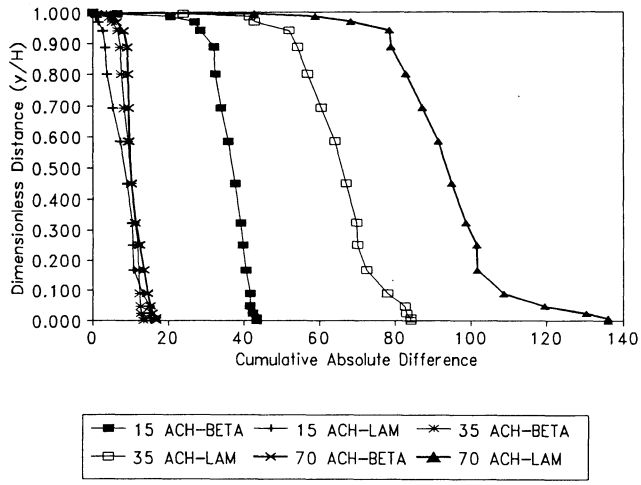


**Figure 9–Cumulative absolute difference between the LBLR model and the Beta and LAM models for ventilating conditions three, six, and four.**

jet spread characteristics. Figure 9 summarizes the cumulative absolute difference between the LBLR model predictions and the BETA and LAM results at x/h = 42.5 (x/L = 0.15). Clearly, the BETA model yielded small differences except at 15 ACH where the cumulative absolute difference exceeded 40% for the 18 vertical grid points. The LAM model was much poorer in matching LBLR-predicted results at 35 and 70 ACH, with cumulative absolute differences between 80 and 135%, respectively. Table 5 compares model performance at 70 ACH. The BETA model agreed with the LBLR model to within 4.2%, with cumulative absolute differences of 16.8%, while the LAM model yielded differences as high as 42.9% with a cumulative absolute difference of 136.1%.

## Conclusions

The BETA model, specifically tailored for opposing plane-wall ceiling jets representative of slot-ventilated livestock facilities, was developed and evaluated by comparing predicted axial and AOZ velocity distributions from the LBLR and LAM models. In addition, BETA model results were compared with experimentally measured results from a laboratory scale test chamber. The results support the following conclusions:

- For opposing plane-wall ceiling jets, the predominant gradient in turbulent viscosity is predicted to occur in the vertical direction.
- An effective viscosity defined as a function of $Re_H$ and normalized vertical height from the floor was used to selectively augment the laminar viscosity in the Navier-Stoke's equation and was successful in enabling adequate turbulent flow predictions.
- The BETA model performed essentially as well as the LBLR model; predicted comparisons between BETA and the LBLR models showed negligible differences for ventilating conditions between $Re_H$ of 35,032 and 11,752.
- Comparison with experimentally measured axial velocity decay indicated that the BETA model reproduced the four jet zones as well as the LBLR model.

**Table 5. Difference between predicted vertical jet spread at x/L = 0.15 (m/s) from LBLR model and the predicted results from the BETA and LAM models for ventilating condition four (70 ACH)***

| y/H | LBLR | BETA | Δ% | Σ(Δ%) | LAM | Δ% | Σ(Δ%) |
|---|---|---|---|---|---|---|---|
| 1.000 | 0.000 | 0.000 | 0.0 | 0.0 | 0.000 | 0.0 | 0.0 |
| 0.995 | 0.272 | 0.260 | –1.2 | 1.2 | 0.702 | 42.9 | 42.9 |
| 0.985 | 0.302 | 0.344 | 4.2 | 5.4 | 0.461 | 15.9 | 58.9 |
| 0.968 | 0.263 | 0.272 | 0.9 | 6.3 | 0.168 | –9.5 | 68.4 |
| 0.938 | 0.172 | 0.152 | –2.0 | 8.3 | 0.071 | –10.0 | 78.4 |
| 0.888 | 0.067 | 0.058 | –0.9 | 9.2 | 0.061 | –0.5 | 78.9 |
| 0.801 | 0.012 | 0.011 | –0.1 | 9.3 | 0.051 | 3.9 | 82.8 |
| 0.693 | –0.004 | –0.006 | –0.2 | 9.4 | 0.039 | 4.4 | 87.1 |
| 0.585 | –0.014 | –0.017 | –0.3 | 9.8 | 0.027 | 4.1 | 91.3 |
| 0.447 | –0.025 | –0.031 | –0.6 | 10.3 | 0.011 | 3.6 | 94.9 |
| 0.323 | –0.036 | –0.046 | –1.0 | 11.4 | 0.001 | 3.7 | 98.6 |
| 0.250 | –0.039 | –0.051 | –1.2 | 12.5 | –0.011 | 2.8 | 101.5 |
| 0.166 | –0.041 | –0.052 | –1.1 | 13.7 | –0.039 | 0.2 | 101.7 |
| 0.088 | –0.036 | –0.046 | –0.9 | 14.6 | –0.106 | –7.0 | 108.6 |
| 0.047 | –0.032 | –0.040 | –0.7 | 15.3 | –0.141 | –10.9 | 119.5 |
| 0.023 | –0.028 | –0.033 | –0.6 | 15.9 | –0.137 | –10.9 | 130.4 |
| 0.008 | –0.012 | –0.021 | –1.0 | 16.8 | –0.068 | –5.6 | 136.1 |
| 0.0000 | 0.000 | 0.000 | 0.0 | 16.8 | 0.000 | 0.0 | 136.1 |

* Percent difference (Δ%) and cumulative absolute difference [ Σ(Δ%)] are defined by eqs. 10 and 11.

## Future Research Needs

The results presented in this study are limited to the ventilating conditions shown in table 1 with the experimental apparatus shown in figure 3. To provide further confidence in the proposed model, experimental data collected in a full-scale facility is needed. Velocity distributions, including the air-jet region, are needed as a database for a model of the type shown in this study and for future models. A model, used with confidence, will provide an invaluable research tool for investigating alternative ventilation designs, and for investigating the influences of ventilation changes on the thermal and air quality environments in livestock facilities. A careful experimental database is required before confidence can be attained.

## References

Adre, N. and L. D. Albright. 1994. Criterion for establishing similar air flow patterns (isothermal) in slotted-inlet ventilated enclosures. *Transactions of the ASAE* 37(1):235-250.

ASHRAE. 1993. *Handbook of Fundamentals*. Atlanta, Ga.: ASHRAE.

Awbi, H. B. 1991. *Ventilation of Buildings*. New York: E & FN Spon, Publishers.

Choi, H. L., L. D. Albright and M. B. Timmons. 1987. Air velocity and contaminant distribution in a slot-ventilated enclosure. ASAE Paper 87-4036. St. Joseph, Mich.: ASAE.

————. 1990. An application of the k–ε turbulence model to predict how a rectangular obstacle in a slot-ventilated enclosure effects air flow. *Transactions of the ASAE* 33(1):274-281.

Choi, H. L., L. D. Albright, M. B. Timmons and Z. Warhaft. 1988. An application of the k-epsilon turbulence model to predict air distribution in a slot-ventilated enclosure. *Transactions of the ASAE* 31(6):1804-1813.

Harlow, F. H. and P. I. Nakayama. 1967. Turbulence transport equations. *Phys. of Fluids* 10(11).

Hoff, S. J., K. A. Janni and L. D. Jacobson. 1992. Three-dimensional buoyant turbulent flows in a scaled model, slot-ventilated, livestock confinement facility. *Transactions of the ASAE* 35(2):671-686.

————. 1995. Evaluating the performance of a low Reynold's number turbulence model for describing mixed-flow airspeed and temperature distributions. *Transactions of the ASAE* 38(5):1533-1541.

Janssen, J. and K. Krause. 1988. Numerical simulation of airflow in mechanically ventilated animal houses. In *Proc., Building Systems: Room Air and Air Contaminant Distribution,* ed. L. L. Christianson, 131-135. 5-8 December.

Kays, W. M. and M. E. Crawford. 1980. *Convective Heat and Mass Transfer,* 2nd Ed. New York: McGraw-Hill.

Kuehn, T. H. 1990. Personal communications based on past numerical modeling experiences. Mechanical Engineering Dept., Univ. of Minnesota.

Lam, C. K. J. and K. A. Bremhorst. 1981. Modified form of the k-ε model for predicting wall turbulence. *J. of Fluids Eng.* 103:456-460.

Launder, B. E. and D. B. Spalding. 1972. *Mathematical Models of Turbulence.* New York: Academic Press.

————. 1974. The numerical computation of turbulent flows. *Computer Methods in Appl. Mech. Eng.* 3:269-289.

Patanker, S. V. and D. B. Spalding. 1970. *Heat and Mass Transfer in Boundary Layers.* London, England: Intertext Books.

————. 1972. A calculation procedure for heat, mass and momentum transfer in three-dimensional parabolic flows. *Int. J. of Heat and Mass Transfer* 15:1787-1806.

Patankar, S. V. 1980. *Numerical Heat Transfer and Fluid Flow.* New York: Hemisphere.

Patel, V. C., W. Rodi and G. Scheuerer. 1985. Turbulence models for near-wall and low Reynold's number flows: A review. *AIAA* 23(9):1308-1319.

Timmons, M. B., L. D. Albright, R. B. Furry and K. E. Torrance. 1980. Experimental and numerical study of air movement in slot-ventilated enclosures. *ASHRAE Transactions* 86(Part 1):221-240.

## NOMENCLATURE

| | |
|---|---|
| $A_\mu$ | constant used in LBLR model (= 0.0165) |
| $A_t$ | constant used in LBLR model (= 20.5) |
| $A_{c1}$ | constant used in LBLR model (= 0.05) |
| ACH | chamber air exchanges per hour ($h^{-1}$) |
| AOZ | animal occupied zone (defined as y/H = 0.05) |
| $c_\mu$ | constant used for turbulent viscosity (= 0.09) |
| $c_1$ | constant used in k-equation (= 1.44) |
| $c_2$ | constant used in e-equation (= 1.92) |
| $C_d$ | coefficient of discharge (= 0.60) |
| $f_\mu$ | LBLR damping function for turbulent viscosity |
| $f_1$ | viscous dissipation auxiliary relation |
| $f_2$ | viscous dissipation auxiliary relation |
| g | gravitational constant (9.81 m/s$^2$) |
| $h_{model}$ | chamber slot height modeled (m) |
| $h_{physical}$ | actual chamber slot height (m) |
| H | building height (= 0.45 m) |
| J | Jet Momentum Number (dimensionless) |
| k | turbulent kinetic energy (m$^2$/s$^2$) |
| L | building (and inlet slot) length (= 1.22 m) |
| P | calculated pressure (Pa) |
| p | static pressure (Pa) |
| Q | inlet ventilation rate (m$^3$/s) |
| $R_k$ | turbulent Reynold's Number (dimensionless) |
| $R_t$ | turbulent Reynold's Number (dimensionless) |
| $Re_h$ | Reynold's Number based on actual inlet slot height (dimensionless) |
| $Re_H$ | Reynold's Number based on building height (dimensionless) |
| $S_\phi$ | generalized source term (per unit volume-time) |
| $U_{in}$ | inlet velocity (m/s) |
| V | building volume (= 0.98 m$^3$) |
| W | building width (= 1.78 m) |
| y+ | dimensionless distance from a solid boundary |
| u, v, w | velocity components in x, y, and z directions (m/s) |
| x, y, z | coordinate directions (m) |

### GREEK SYMBOLS

| | |
|---|---|
| $\beta$ | augmented viscosity ($\mu_t/\mu_l$) |
| $\rho$ | density (kg/m$^3$) |
| $\varepsilon$ | viscous dissipation of turbulent energy (m$^2$/s$^3$) |
| $\mu_l$ | laminar viscosity (kg/m-s) |
| $\mu_t$ | turbulent viscosity (kg/m-s) |
| $\mu_{eff}$ | effective viscosity (= $\mu_l + \mu_t$), (kg/m-s) |
| $\mu'_{eff}$ | effective viscosity used in BETA model (kg/m-s) |
| $\upsilon$ | kinematic viscosity (m$^2$/s) |
| $\Gamma_\phi$ | generalized diffusion coefficient (per m-s) |
| $\sigma$ | Prandtl or Schmidt Number (dimensionless) |

### SUBSCRIPTS

| | |
|---|---|
| eff | effective property (laminar plus turbulent) |
| i, j, k | cartesian-tensor notation (1 = x, 2 = y, and 3 = z) |
| l | laminar component |
| ref | property evaluated using reference (inlet) conditions |
| t | turbulent component |